Cell

Neurofibromin Regulation of ERK Signaling Modulates GABA Release and Learning

Yijun Cui,[1] Rui M. Costa,[1,2] Geoffrey G. Murphy,[1,3] Ype Elgersma,[1,4] Yuan Zhu,[5] David H. Gutmann,[6] Luis F. Parada,[7] Istvan Mody,[8] and Alcino J. Silva[1,*]

[1]Departments of Neurobiology, Psychiatry, and Psychology, Brain Research Institute, University of California, Los Angeles, Los Angeles, CA 90095, USA
[2]Laboratory for Integrative Neuroscience, National Institute on Alcohol Abuse and Alcoholism, National Institutes of Health, 5625 Fishers Lane, Room TS-20D, MSC 9411, Bethesda, MD 20852, USA
[3]Department of Molecular and Integrative Physiology, University of Michigan, Ann Arbor, MI 48109, USA
[4]Department of Neuroscience, Erasmus MC, Dr. Molewaterplein 50, PO Box 2040, 3000 CA Rotterdam, The Netherlands
[5]Departments of Internal Medicine and Cell and Developmental Biology, University of Michigan Medical School, Ann Arbor, MI 48109, USA
[6]Department of Neurology, Washington University School of Medicine, St. Louis, MO 63110, USA
[7]Department of Developmental Biology, University of Texas Southwestern Medical Center, Dallas, TX 75235, USA
[8]Departments of Neurology and Physiology, University of California, Los Angeles, Los Angeles, CA 90095, USA
*Correspondence: silvaa@mednet.ucla.edu
DOI 10.1016/j.cell.2008.09.060

SUMMARY

We uncovered a role for ERK signaling in GABA release, long-term potentiation (LTP), and learning, and show that disruption of this mechanism accounts for the learning deficits in a mouse model for learning disabilities in neurofibromatosis type I (NF1). Our results demonstrate that neurofibromin modulates ERK/synapsin I-dependent GABA release, which in turn modulates hippocampal LTP and learning. An *Nf1* heterozygous null mutation, which results in enhanced ERK and synapsin I phosphorylation, increased GABA release in the hippocampus, and this was reversed by pharmacological downregulation of ERK signaling. Importantly, the learning deficits associated with the *Nf1* mutation were rescued by a subthreshold dose of a GABA$_A$ antagonist. Accordingly, Cre deletions of *Nf1* showed that only those deletions involving inhibitory neurons caused hippocampal inhibition, LTP, and learning abnormalities. Importantly, our results also revealed lasting increases in GABA release triggered by learning, indicating that the mechanisms uncovered here are of general importance for learning.

INTRODUCTION

Previous studies had implicated ERK signaling in learning and long-term potentiation (LTP), a synaptic plasticity mechanism thought to underlie learning and memory. This signaling pathway is activated during both LTP induction and learning, and decreases in its activity result in both LTP and learning deficits (Atkins et al., 1998; English and Sweatt, 1996, 1997; Selcher et al., 1999). ERK signaling is involved in a number of learning tasks, including associative fear conditioning (Atkins et al., 1998), spatial learning (Selcher et al., 1999), and conditioned place preference (Gerdjikov et al., 2004). Likewise, ERK signaling in excitatory neurons is thought to modulate several forms of LTP (Chen et al., 2006; Kelleher et al., 2004; Kushner et al., 2005).

Neurofibromin, a *Ras G*PTase-*a*ctivating *p*rotein (RasGAP) encoded by the neurofibromatosis type I (NF1) gene (Martin et al., 1990; Xu et al., 1990), is thought to modulate Ras/ERK signaling, LTP, and learning in mice (Costa et al., 2002; Li et al., 2005). The NF1 gene is expressed in neurons, astrocytes, Schwann cells, and oligodendrocytes, as well as in many other nonneural cell types (Lynch and Gutmann, 2002). In patients, mutations of the NF1 gene cause learning disabilities and other cognitive symptoms (North, 2000). Visual-spatial problems are among the most common cognitive deficits detected in NF1 patients (Dilts et al., 1996). Interestingly, mice heterozygous for a null mutation of the *Nf1* gene (*Nf1$^{+/-}$*) also have spatial learning problems (Silva et al., 1997). Pharmacological or genetic approaches that reverse the enhancement in ERK signaling in *Nf1$^{+/-}$* mice also reverse their LTP and spatial learning deficits (Costa et al., 2002; Li et al., 2005). However, these studies did not reveal how the increases in Ras/ERK signaling observed in the *Nf1$^{+/-}$* mice led to changes in inhibition and deficits in LTP and learning.

Here, we demonstrate a role for ERK signaling in GABA release, LTP, and learning and show that disruption of this mechanism accounts for the learning deficits in an animal model of NF1. We show that the learning deficits of *Nf1$^{+/-}$* mice are due to increases in ERK activation that lead to higher levels of synapsin I phosphorylation, greater GABA release, and consequently to LTP and learning deficits.

RESULTS

Neurofibromin in Inhibitory Neurons Modulates Learning

To investigate the mechanism responsible for the learning deficits associated with the $Nf1^{+/-}$ mutation, we tested learning in mice with heterozygous Cre-mediated deletions of the $Nf1$ gene in key cell types in the brain. To generate lines with cell-type-specific Cre-mediated deletions, we crossed a mouse line with the $Nf1$ exons 31 and 32 flanked by lox P sites ($Nf1^{floxed}$) (Zhu et al., 2001) with mice expressing Cre recombinase under the control of cell-type-specific promoters: synapsin I promoter (Zhu et al., 2001), GFAP promoter (Bajenaru et al., 2002), αCaMKII promoter (Chen et al., 2006), and Dlx5/6 promoter (Stenman et al., 2003). Therefore, the resulting mice included deletions of $Nf1$ in the following cell types: both excitatory and inhibitory neurons ($Nf1^{syn\ I}$; with synapsin I-Cre), forebrain GABAergic neurons ($Nf1^{Dlx5/6}$; with Dlx5/6-cre), forebrain pyramidal neurons ($Nf1^{αCaMKII}$; with αCaMKII-Cre), and most astrocytes ($Nf1^{GFAP}$; with GFAP-Cre).

To confirm the Cre-mediated deletions, we performed western blot analyses of neurofibromin levels in mice with homozygous Cre-mediated deletions. The results show that neurofibromin levels are reduced in the hippocampus (CA1 region) of the following mice with Cre-mediated homozygous deletions: $Nf1^{syn\ I-/-}$, $Nf1^{Dlx5/6-/-}$, and $Nf1^{αCaMKII-/-}$ (Figure S1 available online). In contrast, The $Nf1^{GFAP-/-}$ mice do not show significant neurofibromin deletion (Figure S1). However, detection of the $Nf1$ deletion in these mice was difficult because the $Nf1$ gene is expressed at low levels in astrocytes of adult mice (Zhu et al., 2001). It is important to note that not all GFAP-Cre lines show astrocyte-specific deletion (Zhuo et al., 2001). However, the line we used appears to restrict deletion to astrocytes (Bajenaru et al., 2002). This could be because of the embryonic date when Cre is first expressed in these two lines (Hegedus et al., 2007).

NF1 patients have visual-spatial cognitive deficits (Dilts et al., 1996), and previous studies showed that the $Nf1^{+/-}$ mice have deficits in spatial learning (Morris water maze) (Silva et al., 1997), a task known to be sensitive to hippocampal lesions (Morris et al., 1982). Thus, the four lines of conditional mutants and controls were trained in the Morris water maze. As controls, we used each of the Cre lines, heterozygous $Nf1^{floxed}$ ($Nf1^{floxed/+}$), and wild-type (WT) mice. No differences were observed between the four conditional mutant lines and their controls in performance on visible platform (Figure S2), floating (continuous immobility for more than 10 s during entire training), thigmotaxic behavior (swimming within 2 cm of pool wall; hug time during day 7 probe trial), or swimming speed during the day 7 probe trial (Table S1). Similarly, a comparison among all groups found no differences in the time mice took to find the platform during training (Figure S3). This is not surprising since this measure is known to be very insensitive to changes in spatial learning (Brandeis et al., 1989). After 7 days of training, the mice were tested in a probe trial, a very sensitive measure of spatial learning (D'Hooge and De Deyn, 2001; Lindner, 1997). The control lines (Table S2), as well as the $Nf1^{αCaMKII+/-}$ and the $Nf1^{GFAP+/-}$ mice, spent more time searching in the quadrant where the plat-
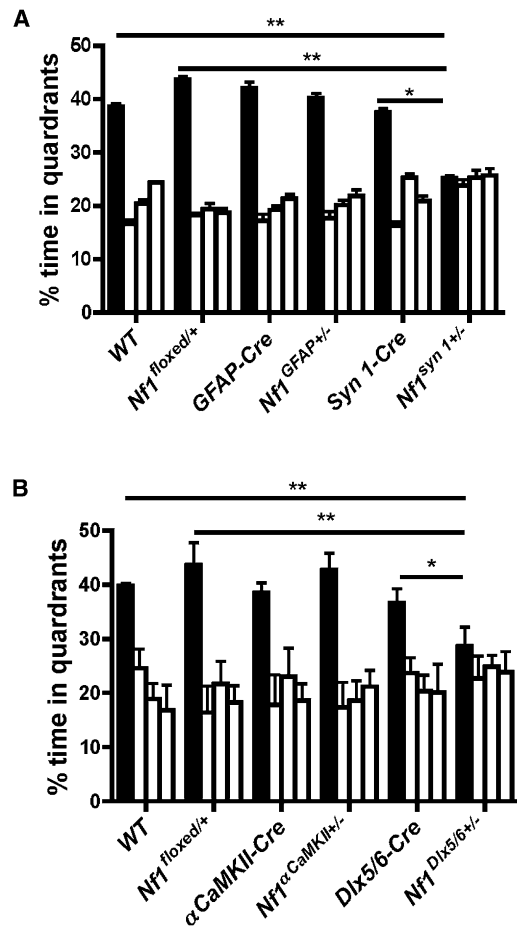
Figure 1. Cre Deletions of the Neurofibromin Gene in Inhibitory Neurons Cause Learning Deficits

(A) $Nf1^{syn\ I+/-}$ mice (n = 13), $Nf1^{GFAP+/-}$ mice (n = 12), and their littermates controls (WT, n = 16; $Nf1^{floxed/+}$, n = 15; $syn\ I$-cre, n = 14; and GFAP-Cre, n = 11) were trained with two trials per day in the Morris water maze. A probe trial conducted after 7 days of training revealed that $Nf1^{syn\ I+/-}$ mice showed no preference for the target quadrant, but $Nf1^{GFAP+/-}$ mice and their littermates did [$F_{(3, 48)} = 0.045$, $p = 0.987$ and $F_{(3, 41)} = 7.873$, $p < 0.001$ for $Nf1^{syn\ I+/-}$ and $Nf1^{GFAP+/-}$ mice, respectively; one-way ANOVA]. Since the $Nf1^{syn\ I+/-}$ and $Nf1^{GFAP+/-}$ are in the same genetic background, the same group of WT and $Nf1^{floxed/+}$ mice (including littermates of $Nf1^{syn\ I+/-}$ and $Nf1^{GFAP+/-}$ mice) were used as controls.

(B) The distribution of target quadrant occupancy during the day 7 probe trial showed that $Nf1^{Dlx5/6+/-}$ mice (n = 8) had no preference for the target quadrant, but $Nf1^{αCaMKII+/-}$ mice (n = 8) and their littermate controls (WT, n = 8; $Nf1^{floxed/+}$, n = 7; Dlx5/6-cre, n = 7; and αCaMKII-Cre, n = 8) searched selectively in the target quadrant [$F_{(3, 28)} = 12.102$, $p < 0.001$ and $F_{(3, 28)} = 0.458$, $p = 0.7141$ for $Nf1^{αCaMKII+/-}$ and $Nf1^{Dlx5/6+/-}$ mice, respectively; one-way ANOVA]. The same WT and $Nf1^{floxed/+}$ mice were used as controls because $Nf1^{Dlx5/6+/-}$ and $Nf1^{αCaMKII+/-}$ mutations were on the same genetic background. The figures shows % search times for each of the four quadrants: target (in black), adjacent left, opposite, and adjacent right quadrants (in that order).

Error bars indicate ± SEM. All statistical comparisons are presented in Tables S2 and S3.

form was during training (training quadrant) than in the other quadrants (Figure 1 and Figure S4). Surprisingly, even mice with an αCaMKII-Cre-mediated homozygous deletion of $Nf1$

($Nf1^{\alpha CaMKII-/-}$) showed normal spatial learning (Figure S5). In contrast, $Nf1^{syn\ I+/-}$ and the $Nf1^{Dlx5/6+/-}$ mice did not spend more time in the training quadrant than in other quadrants (Figure 1 and Figure S4). Accordingly, these two conditional mutant lines spent less time in the training quadrant than did their controls (Table S3). These data demonstrate that heterozygous $Nf1$ deletions driven by either synapsin I-Cre or Dlx5/6-Cre result in spatial learning deficits. Both of these lines are known to express Cre recombinase in interneurons, an unexpected result suggesting a role for neurofibromin in inhibitory neurons.

Neurofibromin in Inhibitory Neurons Modulates GABA Release

Although previous results suggested that GABA-mediated inhibition is altered in $Nf1^{+/-}$ mice (Costa et al., 2002), the mechanisms were unknown. Therefore, we investigated next a possible role for neurofibromin in GABA-mediated inhibition. We examined both inhibitory and excitatory synaptic inputs to CA1 pyramidal neurons in $Nf1^{+/-}$ mice. We first recorded spontaneous inhibitory postsynaptic currents (sIPSCs) in the present of kynurenic acid (1 mM) and miniature inhibitory postsynaptic currents (mIPSCs) in the presence of kynurenic acid (1 mM) and tetrodotoxin (TTX, 1 μM). The sIPSCs and mIPSCs recorded from $Nf1^{+/-}$ and WT mice showed no difference in amplitude, frequency, rise time, and decay time constant (Figures 2A and 2B and Table S4), suggesting normal GABA-mediated inhibition under baseline conditions. However, there is evidence that during learning inhibitory neurons fire at high frequency (Nitz and McNaughton, 2004), and it is possible that under these conditions inhibition is altered in the $Nf1^{+/-}$ mice. Additionally, studies in excitatory neurons indicated that phosphorylation of an ERK site in synapsin I modulates release in response to high-frequency stimulation (Chi et al., 2003), and a similar mechanism may also regulate release in inhibitory neurons.

Therefore, we compared the mIPSCs of $Nf1^{+/-}$ mice and controls after depolarization of synaptic terminals with high KCl (12.5 mM) in artificial cerebrospinal fluid (ACSF) in the presence of kynurenic acid (1 mM) and TTX (1 μM) to mimic high frequency stimulation. These conditions did not change the relative mIPSC amplitude but resulted in a significant increase in mIPSC frequency in both WT and $Nf1^{+/-}$ mice (Figure 2E). Importantly, the ratio between mIPSC frequency recorded in 12.5 mM KCl versus that in control solution (2.5 mM KCl) was significantly larger in $Nf1^{+/-}$ mice than in their WT littermates (Figure 2C), suggesting that under periods of high-frequency stimulation neurofibromin regulates GABA release. It is important to note that both these electrophysiological results with $Nf1^{+/-}$ mice and our behavioral analysis of Cre-driven $Nf1$ deletions indicate a role for neurofibromin in GABAergic neurons.

We also examined excitatory neurotransmission by recording miniature excitatory postsynaptic currents (mEPSCs), which result from spontaneous glutamate release by CA3 neurons on to CA1 neurons. We observed no significant differences in the properties of mEPSCs between the $Nf1^{+/-}$ mice and controls recorded with 2.5 mM KCl (Table S1). Depolarization of synaptic terminals with high KCl (12.5 mM) in ACSF increased the frequency of mEPSC in both WT and $Nf1^{+/-}$ neurons, but the ratio of mIPSC frequency recorded in 12.5 mM KCl to that in control

solution (2.5 mM KCl) was not significantly different between WT and $Nf1^{+/-}$ neurons (Figures 2D and 2F). Together with our behavioral analysis of Cre-driven deletion, this result indicates that heterozygous deletions of $Nf1$ in excitatory neurons do not alter either synaptic function or learning.

The two $Nf1$ heterozygous conditional mutant lines that showed spatial learning deficits, $Nf1^{syn\ I+/-}$ and $Nf1^{Dlx5/6+/-}$, also showed higher mIPSC frequencies (12.5 mM KCl). In contrast, the conditional lines that did not show behavioral deficits ($Nf1^{GFAP+/-}$ and $Nf1^{\alpha CaMKII+/-}$) also did not reveal changes in mIPSCs in either normal or 12.5 mM KCl ACSF (Figures 2G and 2H). These results demonstrate a critical role for neurofibromin (and by implication ERK signaling) in the regulation of GABA release from interneurons.

## Neurofibromin Regulates ERK-Dependent GABA Release

Neurofibromin is a RasGAP that accelerates the conversion of Ras from an active (GTP bound) to an inactive (GDP bound) state (Xu et al., 1990). Indeed, the $Nf1^{+/-}$ mutation leads to elevated Ras-GTP and hyperactivation of Ras downstream effectors such as ERK in the brain (Guilding et al., 2007; Li et al., 2005). To test whether the increased GABA release we observed in $Nf1^{+/-}$ mice is caused by increased ERK signaling activity, we introduced MEK inhibitors U0126 and PD98095 to the perfusion ACSF bath solution to block the Ras-ERK signaling by inhibiting MEK, an ERK kinase. In ACSF with 12.5 mM KCl, introduction of U0126 reduced the frequency of mIPSCs in $Nf1^{+/-}$ mice to the levels of WTs (Figure 3A). However, U0126 did not appreciably affect the mIPSC frequencies of WT and $Nf1^{+/-}$ mice in 2.5 mM KCl ACSF. Similar results were also obtained with another MEK inhibitor, PD98095. Just as U0126, PD98095 did not affect the mIPSC frequencies of WT and $Nf1^{+/-}$ mice with 2.5 mM KCl ACSF, but it brought the frequency of mIPSCs in $Nf1^{+/-}$ mice to the levels of WTs measured in 12.5 mM KCl (Figure 3B). Taken together, these results demonstrate a novel role for ERK signaling in the regulation of GABA release.

NF1 Regulates Learning-Dependent Synapsin I Phosphorylation

Previous findings indicated that ERK phosphorylation of synapsin I modulates glutamate release under high-frequency activation (Chi et al., 2003), and this could be also a mechanism for how neurofibromin regulates GABA release. Therefore, we characterized ERK activation and ERK-dependent phosphorylation of synapsin I in $Nf1^{+/-}$ mice.

Immunohistochemistry studies in the CA1 region detected an increase in the number of ERK phosphorylation-positive inhibitory neurons in both mutants and controls 30 min after 1 day training protocol in the water maze (five trials). Also, we found that the number of ERK phosphorylation-positive inhibitory neurons was overall higher in $Nf1^{+/-}$ mutants than in controls (Figures 4E and 4F). However, because of the difficulties in quantitating immunocitochemistry data, we next carried out western analysis studies.

We decided to use fear conditioning instead of water maze because this one-trial learning task is known to engage hippocampal function and result in the phosphorylation of both ERK and synapsin I (Atkins et al., 1998; Kushner et al., 2005). Unlike the
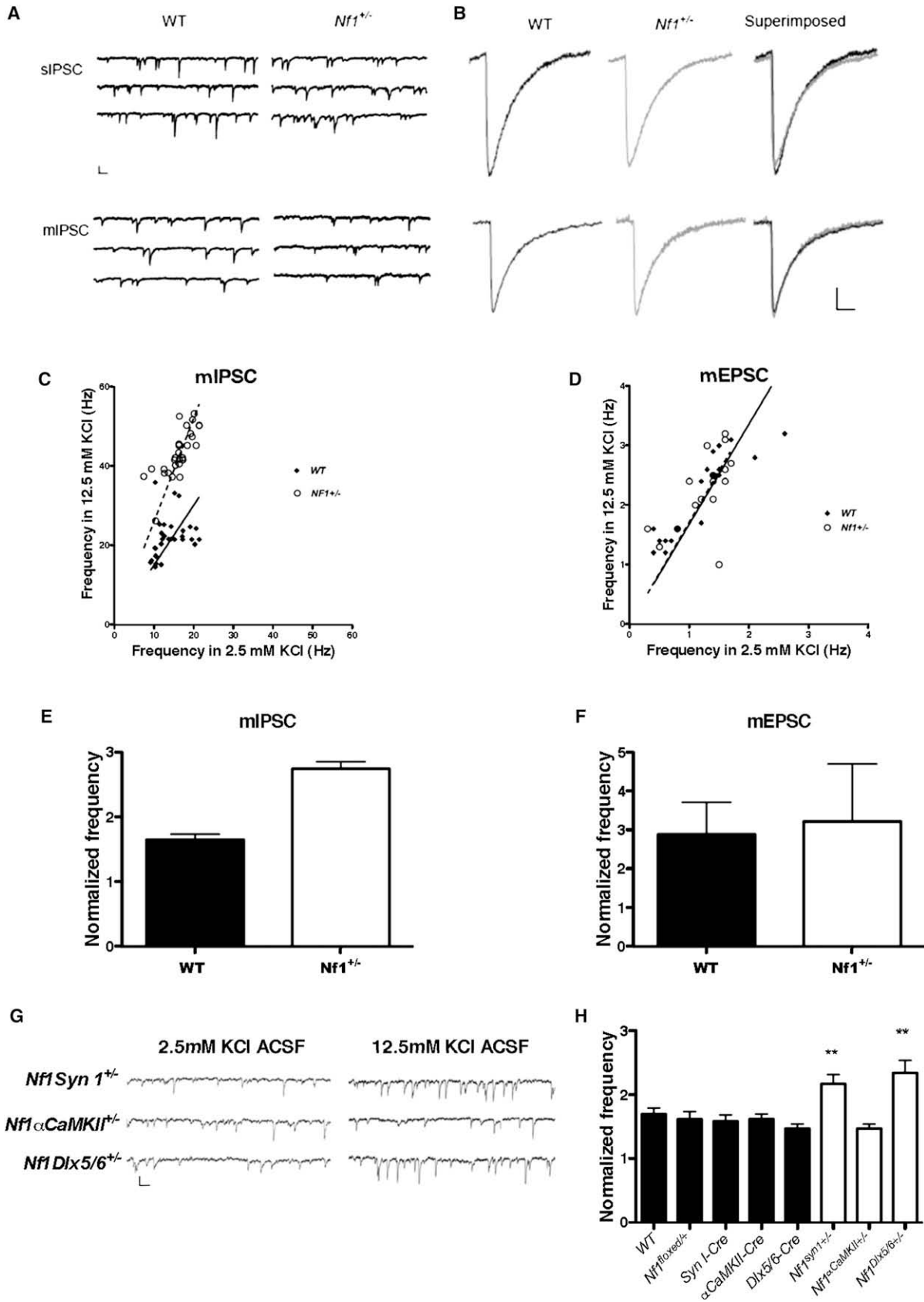
water maze paradigms we used, where learning is distributed through multiple trials taking nearly an hour, in this task learning is concentrated on a single session lasting only 5 min. This allows for better synchronization of learning processes and therefore phosphorylation signals that are more robust and homogeneous. Hippocampal lysates were prepared from $Nf1^{+/-}$ and WT littermates after contextual fear conditioning training. To characterize ERK activation and ERK-dependent phosphorylation of synapsin I in $Nf1^{+/-}$ mutants, we trained mice with a paradigm known to trigger biochemical changes related to conditioning (Kushner et al., 2005) (three foot shocks, each consisting of 0.75 mA for 2 s, that were delivered with a 58 s intershock interval after being placed in a conditioning chamber for 2 min). This strong training paradigm is ideally suited to trigger robust biochemical changes in the hippocampus (Atkins et al., 1998; Kushner et al., 2005) but results in ceiling-level freezing responses that occlude conditioning differences between the genotypes (data not shown). However, consistent with their hippocampal deficits, $Nf1^{+/-}$ mice showed significant impairments in this task when ceiling performances are avoided; $Nf1^{+/-}$ mice and WT controls were given one trial per day for 5 days, and their freezing responses were measured for 30 s on each training day and 24 hr after the last training trial (Figure 4A). Contextual conditioning significantly increased phosphorylation of both ERK and synapsin I (at the ERK site) in WT and $Nf1^{+/-}$ mice. Importantly, the increase in ERK phosphorylation in $Nf1^{+/-}$ mice is higher than that in WT controls (Figures 4B and 4C and Figure S6). As a control, we also used a training procedure that does not trigger contextual learning (Fanselow, 1986); in this procedure, the foot shock is administered immediately after introduction of animals to the training context (immediate shock). This procedure did not cause an increase in ERK phosphorylation in either $Nf1^{+/-}$ or WT mice (data not shown), a result attesting to the learning specificity of ERK phosphorylation triggered with contextual conditioning (e.g., not caused by foot shock). Similarly, $Nf1^{+/-}$ mice showed higher synapsin I phosphorylation than did WT controls (ERK-dependent sites 4/5; Figures 4B and 4D and Figures

S6A and S6C). In contrast, synapsin I phosphorylation at the αCaMKII-dependent site 3 was equivalent in WT and $Nf1^{+/-}$ mice (data not shown). This result indicates that neurofibromin modulates ERK phosphorylation of synapsin I 4/5 sites during learning.

Importantly, the two $Nf1$ heterozygous conditional mutant lines that showed spatial learning deficits, $Nf1^{syn\ I+/-}$ and $Nf1^{Dlx5/6+/-}$, showed higher ERK phosphorylation than WT controls (Figures 4B and 4C). Consistently, $Nf1^{syn\ I+/-}$ and $Nf1^{Dlx5/6+/-}$ also showed higher phosphorylation of ERK-dependent sites 4/5 of synapsin I (Figures 4B and 4D). These results demonstrate that neurofibromin regulates ERK signaling and synapsin I phosphorylation, specifically in inhibitory neurons, a result that provides a mechanistic explanation for neurofibromin's role in GABA release.

Deletion of $Nf1$ Gene from Inhibitory Neurons Leads to LTP Deficits

Previous studies suggested that enhanced GABA-mediated inhibition in the $Nf1^{+/-}$ mice results in deficits in hippocampal LTP (Costa et al., 2002). Thus, we tested whether the Cre deletions that resulted in enhanced inhibition and learning deficits also caused deficits in LTP. Accordingly, we demonstrate that CA1 LTP triggered with a five-theta-burst tetanus was deficient in the $Nf1^{Dlx5/6+/-}$ mutants but not $Nf1^{\alpha CaMKII+/-}$ mutants. Between 40 and 50 min after the tetanus, the $Nf1^{Dlx5/6+/-}$ mice (n = 6 mice) showed 124.5% ± 4.5% potentiation and the $Nf1^{\alpha CaMKII+/-}$ mouse knockouts (n = 9 mice) showed 142.1% ± 6.7% potentiation, whereas WT mice (n = 6 mice) showed 148.6% ± 4.1% (Figure 5). These results show that deletion of $Nf1$ specifically in inhibitory neurons leads to LTP deficits, confirming that the synaptic plasticity deficits of these mutants are caused by increases in inhibitory function.

The Learning Deficits of $Nf1^{+/-}$ Mice Can Be Reversed by Decreasing GABA-Mediated Inhibition

The results described above suggest that the deletion of neurofibromin from inhibitory neurons but not astrocytes or excitatory

---

Figure 2. Increased mIPSC Frequency in $Nf1^{+/-}$ Mutants in High KCl

(A) Representative traces of sIPSCs and mIPSCs recorded from CA1 pyramidal neurons of WT and $Nf1^{+/-}$ mice with normal ACSF (2.5 mM KCl). Calibration: 100 ms and 100 pA.

(B) Average of more than 100 events of sIPSCs or mIPSCs from WT or $Nf1^{+/-}$ neurons. Calibration: 5 ms and 10 pA.

(C and D) Frequency of mIPSCs and mEPSCs recorded in normal and high K+ ACSF. The individual points represent recordings from different neurons. Solid black squares represent WT, and open squares represent $Nf1^{+/-}$ neurons. Solid lines (WT) and dashed lines ($Nf1^{+/-}$) represent the change ratio of the mIPSC or mEPSC frequency of neurons in 12.5 mM KCl versus 2.5 mM KCl ACSF. High KCl (12.5 mM) in ACSF resulted in a significant increase in mIPSC frequency in both WT and $Nf1^{+/-}$ mice (WT: 13.89 ± 0.69 Hz versus 21.98 ± 0.95 Hz, n = 30, paired t test, t = 8.306, p < 0.001; $Nf1^{+/-}$: 16.26 ± 0.65 Hz versus 43.21 ± 1.11 Hz, n = 29, t = 36.525, p < 0.001) (C). High KCl (12.5 mM) in ACSF increased the frequency of mEPSC in both WT (1.15 ± 0.14 Hz in normal ACSF and 2.12 ± 0.17 Hz in ACSF with 12.5 mM KCl, n = 19, paired t test, t = −13.585, p < 0.001) and $Nf1^{+/-}$ (1.25 ± 0.104 Hz in normal ACSF and 2.25 ± 0.16 Hz in ACSF with 12.5 mM KCl, n = 16, paired t test, t = −7.906, p < 0.001) (D).

(E and F) Comparison of normalized mIPSC and mEPSC frequencies in WT and $Nf1^{+/-}$. The ratio of mIPSC frequency recorded in high KCl to that in control solution was significantly larger in $Nf1^{+/-}$ mice (2.76 ± 0.34, n = 29) than in their WT littermates (1.65 ± 0.229, n = 30) (t = 7.906; p < 0.001) (E). The ratio of mEPSC frequency recorded in 12.5 mM KCl to that in control solution was not significantly different between WT and $Nf1^{+/-}$ neurons (2.12 ± 0.15, n = 19 in WT and 2.03 ± 0.24 n = 16, in $Nf1^{+/-}$, Student's t test, t = 0.294, p = 0.7708) (F).

(G) Representative traces of mIPSCs recorded from CA1 pyramidal neurons of WT and Cre-mediated $Nf1$ mutant mice with normal ACSF (2.5 mM KCl) and 12.5 mM KCl ACSF. Calibration: 50 ms and 10 pA.

(H) Normalized frequency changes of miniature IPSCs recorded from CA1 pyramidal neurons in 12.5 mM KCl versus 2.5 mM KCl ACSF of different $Nf1$ mice with Cre-driven deletions (WT, n = 20; $Nf1^{floxed/+}$, n = 19; Syn-Cre, n = 14; αCaMKII-Cre, n = 18; Dlx5/6-Cre, n = 13; $Nf1^{syn\ I+/-}$, n = 15; $Nf1^{\alpha CaMKII+/-}$, n = 15; and $Nf1^{Dlx5/6+/-}$, n = 14). $Nf1^{syn\ I+/-}$ and $Nf1^{Dlx5/6+/-}$ showed higher mIPSC frequencies than the WT when the KCl concentration in ACSF was 12.5 mM KCl (WT: 13.52 ± 0.35 Hz versus 24.31 ± 0.71 Hz; $Nf1^{syn\ I+/-}$: 15.27 ± 0.62 Hz versus 41.26 ± 0.37 Hz; $Nf1^{Dlx5/6+/-}$: 12.46 ± 0.42 Hz versus 35 ± 0.51 Hz; the first value listed for each mutant line is for 2.5 mM and the second is for 12.5 mM KCl). In contrast, mIPSCs in $Nf1^{GFAP+/-}$ and $Nf1^{\alpha CaMKII+/-}$ mice, as well as in all control lines, did not differ from WT mice in either normal or 12.5 mM KCl ACSF.

Error bars indicate ± SEM (E, F, and H).
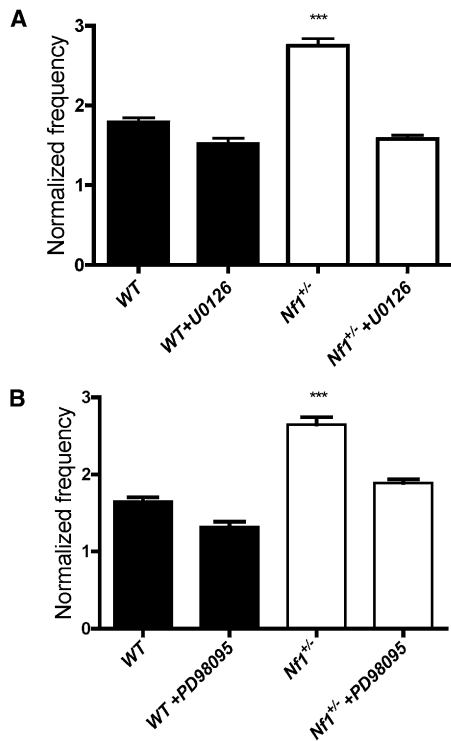
Figure 3. Increased mIPSC Frequency in *Nf1*^{+/−} Mice Is Reversed by MEK Inhibitors

(A) Increased mIPSC frequency caused by high K^{+} ACSF perfusion is reversed by the MEK inhibitor U0126 (normalized frequency: WT without U0126, 1.65 ± 0.058; WT with U0126, 1.32 ± 0.063; *Nf1*^{+/−} without U0126, 2.65 ± 0.082; *Nf1*^{+/−} with U0126, 1.89 ± 0.067; $p > 0.05$ for WT with U0126 versus *Nf1*^{+/−} with U0126).

(B) Increased mIPSC frequency caused by high K+ ACSF perfusion is reversed by the MEK inhibitor PD 98095 (normalized frequency: WT without PD98095, 1.79 ± 0.057; WT with PD98095, 1.52 ± 0.069; *Nf1*^{+/−} without PD98095, 2.75 ± 0.09; *Nf1*^{+/−} with PD98095, 1.58 ± 0.047; $p > 0.05$ for WT with PD98095 versus *Nf1*^{+/−} with PD98095).

Error bars indicate ± SEM.

neurons disrupt spatial leaning and memory. To test whether the learning deficits of these mice are due to enhancements in GABA-mediated inhibition, we used picrotoxin, a GABA_A receptor antagonist. WT and *Nf1*^{+/−} mice were injected intraperitoneally once a day for 3 days before the first training day, and then 30 min before daily training with either saline or 0.01 mg per Kg (body mass) picrotoxin. As before, mice were trained with two trials per day in the Morris water maze. Spatial memory was assessed in a probe trial (end of training day 7), in which the platform was removed from the pool and the mice were allowed to search for it for 60 s. In all the experiments described next, no differences were observed between genotypes and/or treatments in acquisition, floating, thigmotaxic behavior, or swimming speed (Table S5 and Figure S7). Analysis of the day 7 probe trial showed an interaction between genotype and treatment. Importantly, 0.01 mg/Kg picrotoxin did not affect the searching time of WT mice in the training quadrant. However, *Nf1*^{+/−} mice treated with 0.01 mg/Kg picrotoxin searched significantly longer in the training quadrant than did *Nf1*^{+/−} mice treated with saline and

were indistinguishable from WT mice with or without treatment (Figure 6). Importantly, a higher dose of picrotoxin (0.03 mg/Kg) enhanced learning in both *Nf1*^{+/−} mice and controls (Figure S8). The finding that the learning deficits of *Nf1*^{+/−} mice can be reversed with a dose of picrotoxin (0.01 mg/Kg) that is ineffective in WT shows that these learning deficits can be rescued by decreased GABA-mediated inhibition. All together the results presented here demonstrate a role for ERK signaling in GABA release and learning and suggest a novel approach for treating the learning disabilities associated with NF1.

Spatial Learning Triggers Lasting Increases in GABA Release

The results presented above suggest an unexpected link between GABA release and learning. To test whether spatial learning causes lasting changes in GABA release, we first trained C57BL/6N mice in the water maze. We included three groups: A *learning* group that was given one day of spatial training, a *swimming-only control* group that spent in average the same amount of time in the pool but got no spatial training, and a *cage control* group that was never exposed to any aspect of handling or training. Sixty minutes after training, mice were sacrificed and mIPSCs (2.5 mM KCl) were studied as before (>1 hr slice incubations). Mice in the *learning* group showed higher mIPSC frequency than either the *swimming* group or the *cage controls* (Figure 7). No differences were observed between the *swimming* group and the *cage controls*. In contrast with mIPSP frequency, the amplitude, rise time, and decay time constant were not significantly different between groups (Figure 7). These results indicate that spatial training causes a lasting (>2 hr) increase in GABA release in the hippocampal CA1 region.

DISCUSSION

The results described here uncovered a role for ERK signaling in GABA release, plasticity, and learning. We also show that disruption of this mechanism accounts for the learning deficits associated with NF1. Our results demonstrate that the learning deficits in a mouse model of neurofibromatosis type I are caused by increased hippocampal GABA release, which dampens hippocampal synaptic plasticity and consequently leads to hippocampal-dependent learning deficits. Importantly, we also showed that spatial learning triggers a lasting increase in GABA release, and we demonstrate that neurofibromin modulates ERK-dependent phosphorylation of synapsin I and that this is critical for GABA release, LTP, and learning. Thus, our findings suggest that the mechanisms uncovered in our NF1 studies are of general importance for learning and memory and not just specific to the pathology of NF1.

A key finding reported here is that neurofibromin in inhibitory neurons regulates ERK-dependent phosphorylation of synapsin I and consequently GABA release. First, we reported that *Nf1*^{+/−} mice, as well as mice with either an *Nf1* deletion in inhibitory neurons (*Nf1*[Dlx5/6+/−]) or in inhibitory and excitatory neurons (*Nf1*[Syn I+/−]), showed increased frequency of mIPSCs, a traditional marker of presynaptic effects, without changes in mIPSC amplitude, rise time, or decay constant, three common electrophysiological tags of postsynaptic changes in neurotransmission. In

contrast, deletion of *Nf1* in excitatory neurons (*Nf1$^{\alpha CaMKII+/-}$*) or astrocytes *(Nf1$^{GFAP+/-}$)* did not affect mIPSCs. These results indicate that neurofibromin has a critical role in GABA release. Second, two different MEK inhibitors rescued the increase in mIPSC frequency observed in *Nf1$^{+/-}$* mice, implicating the Ras/MEK/ERK signaling pathway in GABA release. In addition, we showed that MEK inhibition, although less effectively, also affected mIPSC frequency in controls, indicating that these effects are not specific to *Nf1* mutants. However, importantly, the *Nf1$^{+/-}$* mutation did not affect mEPSCs, indicating that neurofibromin does not modulate ERK's role in hippocampal glutamatergic release (Kushner et al., 2005). Previous work had indicated that the ERK signaling pathway modulates learning by regulating postsynaptic LTP mechanisms (Sweatt, 2004). Our results are not in contradiction with these earlier findings, and instead they suggest that other GAPs (Bernards and Settleman, 2004) control ERK signaling in excitatory neurons during learning.

How does neurofibromin/ERK signaling modulate GABA release? Previous reports implicated ERK signaling in synapsin I phosphorylation, vesicle docking, and glutamate release under conditions of high stimulation frequency. Consistent with previous models of synapsin I function in excitatory neurons (Chi et al., 2003), our findings suggest that the higher ERK activation found in inhibitory neurons leads to higher levels of synapsin I phosphorylation and therefore to greater GABA release. We show that behavioral training known to engage the hippocampus (Frankland et al., 1998; Kim and Fanselow, 1992) results in more robust hippocampal ERK phosphorylation and ERK-dependent phosphorylation of synapsin I in *Nf1* mice, including those with the mutation restricted to inhibitory neurons (*Nf1$^{Dlx5/6+/-}$*). Since the deletion in *Nf1$^{Dlx5/6+/-}$* is restricted to inhibitory neurons, we can attribute the increase in ERK and synapsin I phosphorylation to processes in these cells. Additionally, we showed that deletion of the *Nf1* gene in excitatory neurons does not affect ERK, synapsin I phosphorylation, or various measures of glutamate release, indicating that neurofibromin does not play a critical role in the modulation of ERK/synapsin I function in excitatory presynaptic terminals.

Importantly, mutations (*Nf1$^{+/-}$*, *Nf1$^{Dlx5/6+/-}$*, and *Nf1$^{Syn\ I+/-}$*) that affected GABA release also disrupted LTP, demonstrating that the LTP deficits previously reported for *Nf1$^{+/-}$* mice are caused by increased GABA release. Additionally, the very same lines with increased hippocampal GABA release and LTP deficits also showed abnormal learning in a hippocampal-dependent task (i.e., Morris water maze), whereas the *Nf1$^{\alpha CaMKII+/-}$* mice did not show inhibition, LTP, or learning abnormalities. Abnormally high levels of GABA released during learning could result in increased hyperpolarization of excitatory neurons and consequently in deficits in LTP. In contrast, upregulation of the ERK signaling pathway in excitatory neurons leads to enhancements of both LTP and learning in mice (Kushner et al., 2005), whereas downregulation in excitatory neurons leads to LTP and learning deficits (Chen et al., 2006). Altogether these findings demonstrate that ERK signaling in both excitatory and inhibitory neurons is critical for synaptic plasticity and learning.

The results discussed above demonstrate that increases in GABA release can affect learning. But, does learning also affect GABA release? Our results demonstrate that spatial training in the Morris water maze caused a lasting increase in GABA release, a result consistent with the idea that changes in GABAergic function may have a role in orchestrating the circuit changes involved in memory. Although these findings suggest that learning normally involves increases in GABA release, our results demonstrate that the abnormally high GABA release documented for *Nf1$^{+/-}$* mice disrupts LTP and learning.

Our findings also impact the development of treatments for the learning disabilities associated with NF1; we demonstrated that increased GABA release is responsible for the LTP and learning deficits associated with *Nf1$^{+/-}$* mice. This result is consistent with previous findings that GABAergic transmission is important in the regulation of synaptic plasticity and learning (Crestani et al., 2002; Introini-Collison et al., 1994; McElroy and Korol, 2005; Wiltgen et al., 2005). On the basis of our finding that *Nf1* mutants have increased inhibition, we were able to reverse the learning deficits of the *Nf1$^{+/-}$* mice with a dose of a GABA$_A$ antagonist (picrotoxin) that was shown not to enhance learning in WT mice. These results confirm the role of inhibition in the learning deficits associated with NF1 and suggest that safe strategies that decrease GABA-mediated inhibition will be useful for treatment of the learning deficits associated with NF1. It is important to note that GABAergic drugs like picrotoxin have a limited clinical usefulness because of their dangerous convulsant properties. However, it may be possible to use safer GABAergic drugs that preserve the beneficial cognitive effects without the proconvulsant properties (Atack et al., 2006). Interestingly, a recent study also found that changes in GABA inhibition underlie the learning deficits of an animal model of Down syndrome (Kleschevnikov et al., 2004; Rueda et al., 2008), suggesting that GABA inhibition may have a prominent role in the pathophysiology of cognitive disorders.

EXPERIMENTAL PROCEDURES

Mouse Breeding and Genotyping

All animal protocols were approved by the Chancellor's Animal Research Committee of the University of California, Los Angeles and in accordance with National Institutes of Health (NIH) guidelines. In this paper, we used 3- to 6-month-old males and females. Studies with *Nf1$^{+/-}$* mice were performed in 129T2/SvEmsJ-C57BL/6 F1 hybrids. WT littermates were used as controls. The mice with Cre-mediated deletions of the *Nf1* gene (*Nf1$^{Dlx5/6+/-}$*, *Nf1$^{syn\ I+/-}$*, *Nf1$^{CamKII\ +/-}$*, and *Nf1$^{GFAP+/-}$*) were F1 progeny from a cross between the *Nf1$^{floxed/+}$* and the cell-type-specific Cre mice (*synapsin 1-Cre*, *GFAP-Cre*, *αCaMKII-Cre*, and *Dlx5/6-Cre*). The four lines with Cre deletions of the *Nf1* gene (and their controls) were all in a 129T2/SvEmsJ-C57BL/6 F1 hybrid genetic background. Since the four different *Nf1$^{Cre+/-}$* lines share the same genetic background (all in a 129T2/SvEmsJ-C57BL/6 F1 hybrid background), in some experiments we combined WT and *Nf1$^{floxed/+}$* littermates of different conditional mutant lines. The *Nf1$^{Cre-/-}$* mice were F2 progeny of the *Nf1$^{Cre+/-}$* mice. Mouse genotypes were determined by PCR analysis of tail DNA samples as described before. All experiments were carried out with researchers blind to the genotype of the animals tested.

Western Blot Analysis

Immunoblot analyses were performed as described previously (Elgersma et al., 2002). In Figure 4 and Figure S6, tissue was collected 30 min after behavioral training. The primary antibodies used were against NF1 (1:300; Santa Cruz Biotechnology), phospho-ERK p42/p44 and total ERK p42/p44 (1:1000; NEB), β-actin (1:5000; Sigma), synapsin I (1:1000; NEB), and phospho-synapsin I, a gift from P. Greengard (Rockefeller University, New York, NY). Blots
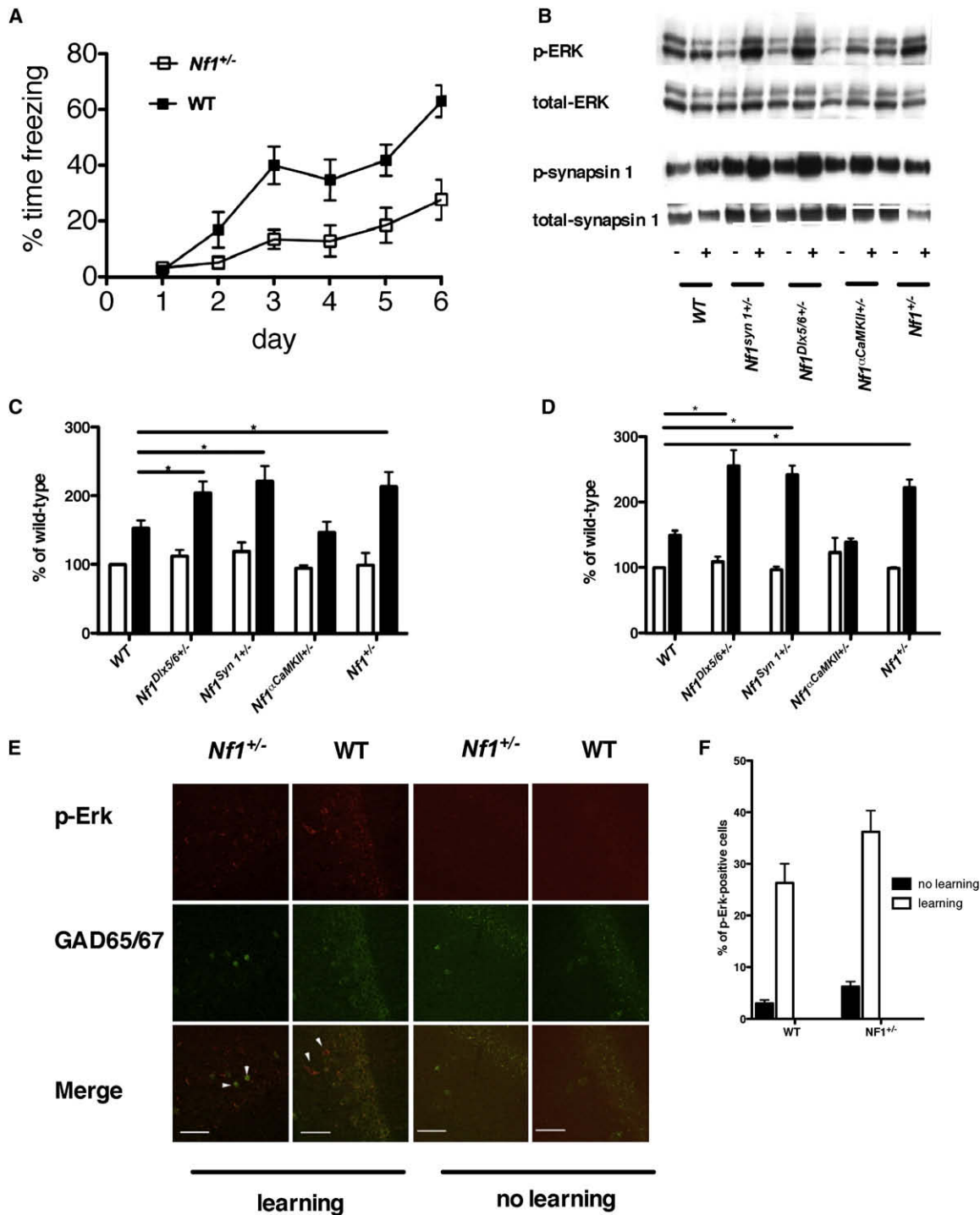
Figure 4. Increased ERK-Dependent Synapsin I Phosphorylation in Cre-Mediated *Nf1* Mutants

(A) *Nf1*$^{+/-}$ mice have deficits in the acquisition of contextual fear conditioning. *Nf1*$^{+/-}$ mice (n = 16) and WT controls (n = 14) were trained with a contextual fear-conditioning protocol using one trial per day for five consecutive days. The average freezing levels during the first 30 s of each training day and 24 hr after the last training trial were plotted. WT mice freeze significantly more compare to WT [$F_{(1,140)}$ = 3.927, p < 0.05].

(B) Contextual conditioning increases the phosphorylation of ERK and synapsin I (sites 4/5). Representative western blots indicating protein bands visualized with antibodies to dually phosphorylated ERK1/2, total ERK1/2, synapsin I at sites 4/5, and total ERK1/2. + denotes contextual conditioning (shocks were delivered during the contextual exposure). − denotes that the no shock was delivered.

(C and D) Quantification of relative phosphorylated ERK1/2, and synapsin I at sites 4/5. For each experiment, both phosphorylated and total MAPK levels were normalized to those observed in the control group of wild-type mice. Three to six mice were in each group.
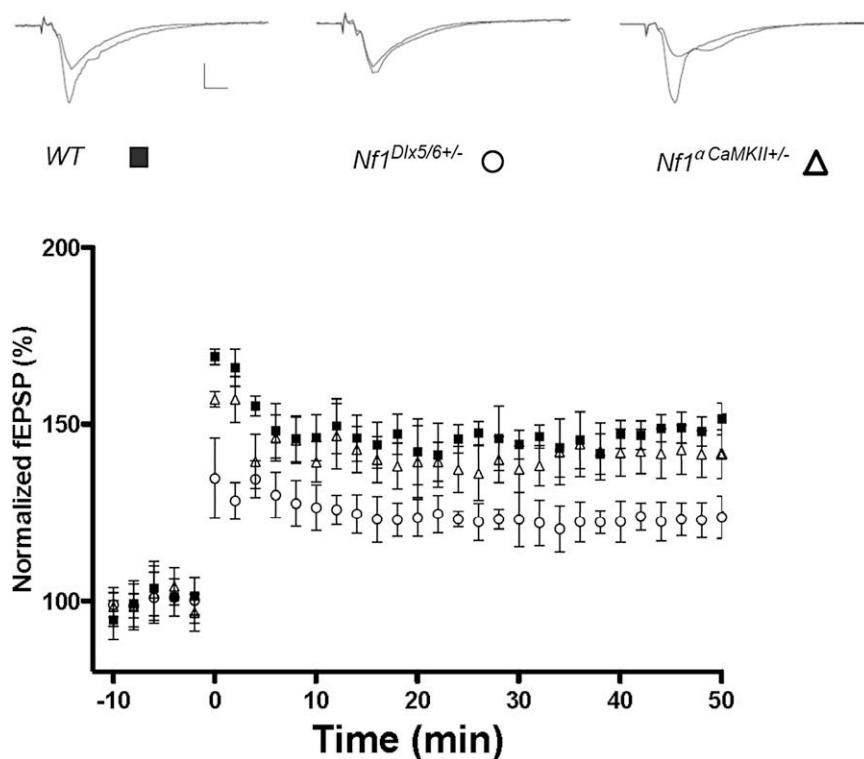
LTP induced by a five-theta-burst tetanus (at 10 min). Each point indicates the field EPSP slope normalized to the average baseline response before the tetanus delivered at time 0. (Solid square, WT; open circle, $Nf1^{Dlx5/6+/−}$; open triangle, $Nf1^{αCaMKII+/−}$.) Between 40 and 50 min after the tetanus, the $Nf1^{Dlx5/6+/−}$ mice (n = 6) showed 124.5% ± 4.5% potentiation, and the $Nf1^{αCaMKII+/−}$ mice (n = 9) showed 142.1% ± 6.7% potentiation, whereas WT mice (n = 6) showed 148.6% ± 4.1% [$F_{(1,10)}$ = 18.713, p < 0.01; $F_{(1,13)}$ = 0.613, p = 0.4477 for $Nf1^{Dlx5/6+/−}$ and $Nf1^{αCaMKII+/−}$, respectively, when compared with WT mice, one-way ANOVA]. Error bars indicate ± SEM.

form was present. So that fatigue could be avoided, training was divided into five sessions (4 min each) with 15 min ITI. Mice in the *cage-control* group were sacrificed immediately after removal from the home cage. Mice from both the *learning* and *swimming-only* groups were sacrificed 60 min after the last session, and mIPSCs (see below) were recorded. In the visible version of water maze, mice were trained to search for a marked platform that was placed at a different location for five trials during 1 day (30 min ITI).

were quantitated with ECL⁺ and the Storm 860 phosphorimager system (Molecular Dynamics, Sunnyvale, CA).

Immunohistochemistry

Immunohistochemistry was performed with confocal microscopy as described previously (Kushner, et al. 2005). The primary antibodies used were against phospho-Thr202/Tyr204 ERK p42/p44 (New England Biolabs) and GAD65/67 (Chemicon). FITC donkey anti-rabbit and cyanine 3 (Cy3) donkey anti-mouse were used as secondary antibodies. Sections were analyzed with a Zeiss LSM 510 confocal laser-scanning microscope with a 40× numerical aperture objective.

Neuronal quantification was performed by counting of cellular FITC fluorescence and cellular Cy3 immunofluorescence.

Behavioral Analysis

The Morris water maze apparatus and procedures were previously described (Costa et al., 2002). Mice were trained with two trials per day for 7 days (30 s intershock interval [ITI]). Probe trials were administered 5 and 7 days after the completion of training. For the studies that looked at inhibition after water maze training, Mice were initially habituated for 7 days (2 min handling and 5 min swimming per day). Mice in the *learning* group were spatial trained with 15 trials (5 min ITI). In each trial, mice were given 30 s on a platform and another 60 s to find the platform (Figure S9). Two mice were excluded from further analysis because of floating. Mice in the *swimming-only* group spent on average the same amount of time as the *learning* group in the pool, but no plat-

The contextual fear-conditioning apparatus was previously described (Anagnostaras et al., 2000). For the experiment in which the acquisition of contextual conditioning was gradually tested in the $Nf1^{+/}$ mutants, the mice were placed in a conditioning chamber for 40 s, after which they were given a single foot shock (0.40 mA, 2 s). Mice were trained with one trial per day for five consecutive days. At the beginning of each training day and 24 hr after the last training trial, the freezing levels were monitored for 30 s with an automated procedure (Anagnostaras et al., 2000).

For the ERK and synapsin I phosphorylation studies after robust contextual conditioning (Chen et al., 2006), mice were placed into a conditioning chamber, and 2 min later three foot shocks (0.75 mA, 2 s) were delivered with a 58 s ITI. Then, mice were allowed to remain in the chamber for an additional 1 min before they were returned to their home cages. Hippocampi were removed 30 min after training for western blot analysis.

All values are reported as mean ± SEM. A two-way ANOVA with repeated measures was used for analysis of the acquisition data from the water maze and freezing levels in the fear conditioning. A single-factor ANOVA was used for analysis of performance in the water maze probe on the percentage time in quadrant. A paired t test was used for analysis of the proximity data and crossing time.

Electrophysiology

Transverse hippocampal slices (400 μm thick) were maintained in a submerged recording chamber perfused with ACSF equilibrated with 95% O_2 and 5% CO_2 at 30°C. The ACSF contained the following: 120 mM NaCl, 2.5 mM

(E) Increased ERK phosphorylation in inhibitory neurons of $Nf1^{+/−}$ and WT mice after Morris water maze training after spatial learning. Double immunofluorescent staining shows phosphorylated ERK (red) in inhibitory neurons (labeled with GAD65/67, green) of both WT and $Nf1^{+/−}$ mice. The arrows point to examples of neurons positive for both GAD65/67 and phosphorylated ERK in the hippocampal CA1 region of WT and $Nf1^{+/−}$ mice. The scale bars represent 50 μm.

(F) Quantification of the relative number of ERK phosphorylation-positive inhibitory neurons in the CA1 region of $Nf1^{+/−}$ mutants and WT controls. The overall number of ERK phosphorylation-positive inhibitory neurons in the CA1 region is higher in $Nf1^{+/−}$ mutant (6.2% ± 2.2%, n = 4) mice than in WT controls (3.0% ± 1.3%, n = 4, t test, p = 0.0414); after five training trials in the Morris water maze, the numbers of ERK phosphorylation-positive inhibitory neurons in the CA1 region increased in both $Nf1^{+/−}$ (36.2% ± 9.21%, n = 5) and WT (26.3% ± 7.43%) mice.
Error bars indicate ± SEM (A, C, D, and F).
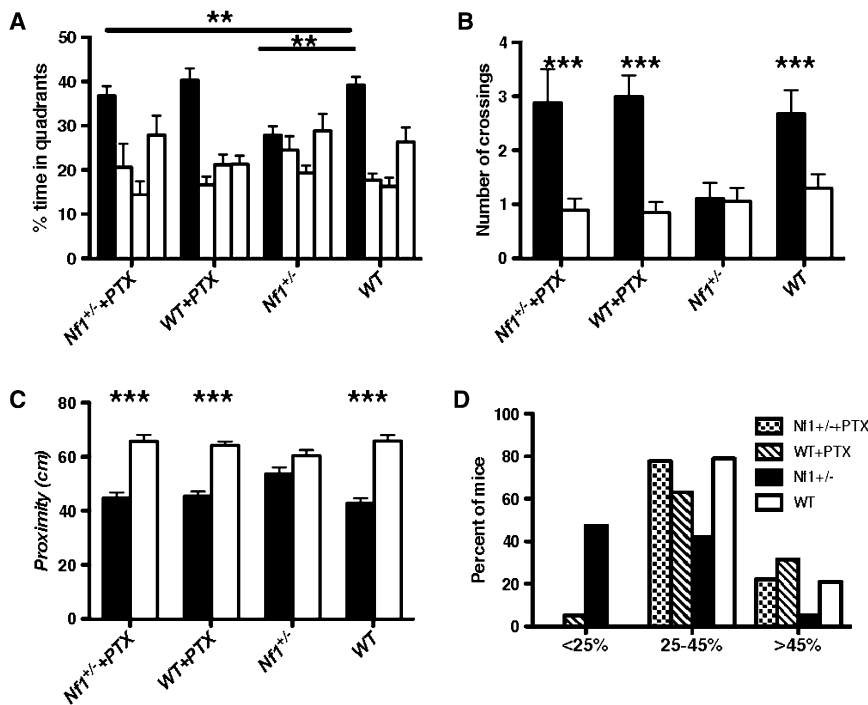
Figure 6. Spatial Learning and Memory Deficits of $Nf1^{+/-}$ Mice Are Reversed by a Subthreshold Dose of Picrotoxin

(A) Mean percentage of time spent in each quadrant during a probe trial. Analysis of the day 7 probe trial showed an interaction between genotype and treatment [$F_{(3,71)} = 7.937$, $p < 0.01$, two-way ANOVA]. The searching time of WT mice in the target quadrant was not affected by 0.01 mg/Kg picrotoxin ($39.23\% \pm 2.20\%$ for WT mice treated with saline versus $40.40\% \pm 2.64\%$ for WT mice treated with picrotoxin).

$Nf1^{+/-}$ mice treated with picrotoxin searched significantly longer in the training quadrant than did $Nf1^{+/-}$ mice treated with saline ($27.94\% \pm 2.05\%$ for $Nf1^{+/-}$ mice treated with saline versus $36.83\% \pm 2.19\%$ for $Nf1^{+/-}$ mice treated with picrotoxin) and were indistinguishable from WT mice with or without treatment. The figure shows % search times for each of the four quadrants: target (in black), adjacent left, opposite, and adjacent right quadrants (in that order).

(B) Number of times the mice crossed the exact position where the platform was during the training (solid bar) compared with the number of crossings in the opposite position in the pool (open bar). The number of crossings of WT mice to the target quadrant was not affected by 0.01 mg/Kg picrotoxin (2.68 ± 0.43 times for WT mice treated with saline versus 3.00 ± 0.39 for WT mice treated with picrotoxin). $Nf1^{+/-}$ mice treated with picrotoxin crossed the platform site more times than did $Nf1^{+/-}$ mice treated with saline (1.11 ± 0.30 for $Nf1^{+/-}$ mice treated with saline versus 2.89 ± 0.63 for $Nf1^{+/-}$ mice treated with picrotoxin) and were indistinguishable from WT mice with or without treatment.

(C) Average proximity to the exact position where the platform was during training (solid bar) compared with proximity to the opposite position in the pool (open bar). The proximity of WT mice in the target quadrant was not affect by 0.01 mg/Kg picrotoxin (42.82 ± 1.84 cm in target quadrant for WT mice treated with saline versus 45.44 ± 1.75 cm in target quadrant for WT mice treated with picrotoxin). $Nf1^{+/-}$ mice treated with picrotoxin searched significantly closer to the platform than did $Nf1^{+/-}$ mice treated with saline (53.69 ± 2.32 cm for $Nf1^{+/-}$ mice treated with saline versus 44.67 ± 2.15 cm for $Nf1^{+/-}$ mice treated with picrotoxin) and were indistinguishable from WT mice with or without treatment.

(D) Distribution of performance of each group of mice in the probe trial. The percentage of mice spending less than 25%, between 25%–45%, and more than 45% of the time in the training quadrant during the day 7 probe trial is plotted for each group (WT, n = 19; $Nf1^{+/-}$, n = 19; WT+PTX, n = 19; N$f1^{+/-}$ +PTX, n = 18). Error bars indicate $\pm$ SEM (A–C).

KCl, 2.5 mM CaCl2, 1.3 mM MgSO4, 1.25 mM NaH2PO4, 26 mM NaHCO3, and 10 mM D-glucose. Field EPSPs (fEPSPs) were recorded with a metallic electrode in CA1 stratum radiatum. The Schaffer collaterals were stimulated with 100 micro s test pulses via a bipolar electrode. The intensity of stimulation was fixed at 60 mA. LTP was induced by a five-theta-burst tetanus stimulation protocol (each burst consists of four pulses at 100 Hz with a 200 ms interburst interval). Responses from the last 10 min block of recordings were compared with ANOVA with Fisher's PLSD for post hoc comparisons.

Whole-cell voltage-clamp recordings (Hajos et al., 2000) with an Axopatch 200B amplifier (Axon Instruments, Foster City, CA) or a 3900A Integrating Patch Clamp Amplifier (Dagan, Minneapolis, MN) were performed for measurement of sIPSCs, mIPSCs, and mEPSCs. All recordings were made from the soma of visually identified CA1 pyramidal neurons. Patch electrodes (3–8 M when filled) were filled with a solution containing the following: 140 mM CsCl, 4 mM NaCl, 1 mM MgCl2, 10 mM HEPES, 0.05 mM ethylene glycol tetraacetic acid (EGTA), 2 mM Mg-ATP, and 0.4 mM Mg-GTP. Whole-cell voltage-clamp recordings were performed at -60 to -70 mV. Series resistance was compensated to 75%–80%. Only recordings during which series resistance changed less than 25% through the whole experiment were analyzed. All recordings were low-pass filtered at 2 kHz and on-line digitized at 10 kHz with a PCI-MIO 16E-4 data-acquisition board (National Instruments, Austin, TX). sIPSCs, mIPSCs, and mEPSCs were measured with in-house data-acquisition and analysis software (Hajos et al., 2000). Data are presented as mean ± SEM. Statistical comparisons of mEPSC data were performed with paired and unpaired t tests and ANOVA.

SUPPLEMENTAL DATA

Supplemental Data include nine figures and five tables and can be found with this article online at http://www.cell.com/supplemental/S0092-8674(08)01296-8.

REFERENCES

Anagnostaras, S.G., Josselyn, S.A., Frankland, P.W., and Silva, A.J. (2000). Computer-assisted behavioral assessment of Pavlovian fear conditioning in mice. Learn. Mem. 7, 58–72.
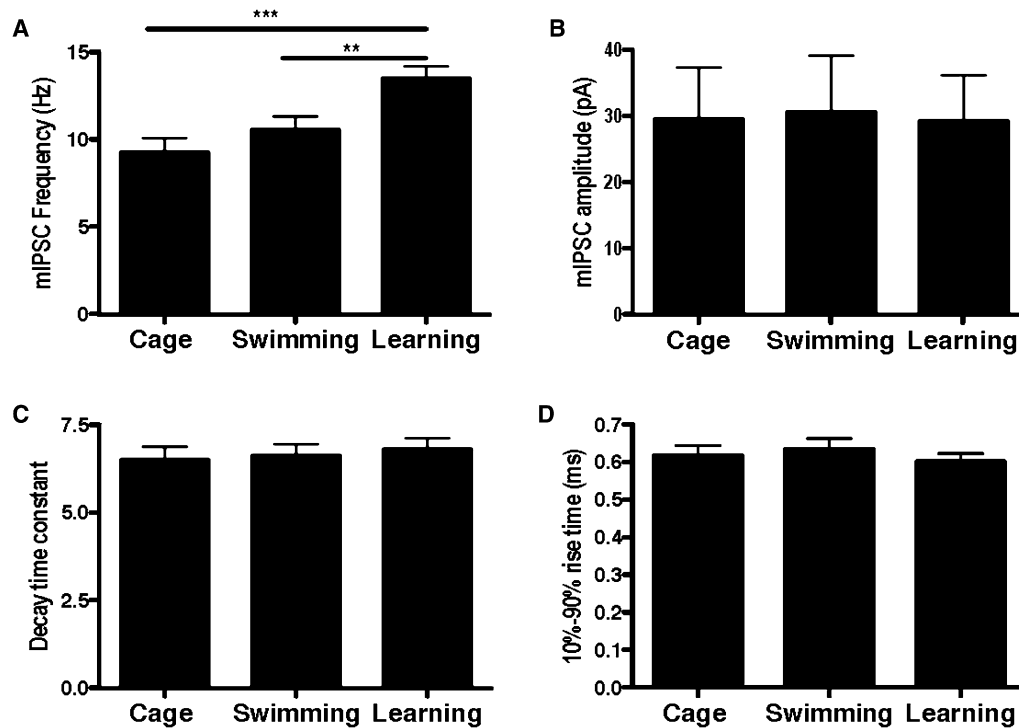
Figure 7. Spatial Learning Increases mIPSC Frequency in Hippocampal CA1 Neurons

One hour after water maze training, mIPSC frequency (A), amplitude (B), decay time constant (C), and 10%–90% rise time (D) of the *learning* group were compared with *swimming control* and *cage control* levels.

(A) mIPSC frequency of the *learning* group was significantly above control levels [$F_{(2, 44)}$ = 8.954, $p < 0.001$, one-way ANOVA; **$p < 0.01$, ***$p < 0.001$].

(B, C, and D) mIPSC amplitude (B), decay time constant(C) and 10%–90% rise time (D) of the *learning* group were not significantly different from control levels. Error bars indicate ± SEM.

Atack, J.R., Bayley, P.J., Seabrook, G.R., Wafford, K.A., McKernan, R.M., and Dawson, G.R. (2006). L-655,708 enhances cognition in rats but is not proconvulsant at a dose selective for alpha5-containing GABAA receptors. Neuropharmacology *51*, 1023–1029.

Atkins, C.M., Selcher, J.C., Petraitis, J.J., Trzaskos, J.M., and Sweatt, J.D. (1998). The MAPK cascade is required for mammalian associative learning. Nat. Neurosci. *1*, 602–609.

Bajenaru, M.L., Zhu, Y., Hedrick, N.M., Donahoe, J., Parada, L.F., and Gutmann, D.H. (2002). Astrocyte-specific inactivation of the neurofibromatosis 1 gene (NF1) is insufficient for astrocytoma formation. Mol. Cell. Biol. *22*, 5100–5113.

Bernards, A., and Settleman, J. (2004). GAP control: Regulating the regulators of small GTPases. Trends Cell Biol. *14*, 377–385.

Brandeis, R., Brandys, Y., and Yehuda, S. (1989). The use of the Morris Water Maze in the study of memory and learning. Int. J. Neurosci. *48*, 29–69.

Chen, A.P., Ohno, M., Giese, K.P., Kuhn, R., Chen, R.L., and Silva, A.J. (2006). Forebrain-specific knockout of B-raf kinase leads to deficits in hippocampal long-term potentiation, learning, and memory. J. Neurosci. Res. *83*, 28–38.

Chi, P., Greengard, P., and Ryan, T.A. (2003). Synaptic vesicle mobilization is regulated by distinct synapsin I phosphorylation pathways at different frequencies. Neuron *38*, 69–78.

Costa, R.M., Federov, N.B., Kogan, J.H., Murphy, G.G., Stern, J., Ohno, M., Kucherlapati, R., Jacks, T., and Silva, A.J. (2002). Mechanism for the learning deficits in a mouse model of neurofibromatosis type 1. Nature *415*, 526–530.

Crestani, F., Keist, R., Fritschy, J.M., Benke, D., Vogt, K., Prut, L., Bluthmann, H., Mohler, H., and Rudolph, U. (2002). Trace fear conditioning involves hippocampal alpha5 GABA(A) receptors. Proc. Natl. Acad. Sci. USA *99*, 8980–8985.

D'Hooge, R., and De Deyn, P.P. (2001). Applications of the Morris water maze in the study of learning and memory. Brain Res. Brain Res. Rev. *36*, 60–90.

Dilts, C.V., Carey, J.C., Kircher, J.C., Hoffman, R.O., Creel, D., Ward, K., Clark, E., and Leonard, C.O. (1996). Children and adolescents with neurofibromatosis 1: A behavioral phenotype. J. Dev. Behav. Pediatr. *17*, 229–239.

Elgersma, Y., Fedorov, N.B., Ikonen, S., Choi, E.S., Elgersma, M., Carvalho, O.M., Giese, K.P., and Silva, A.J. (2002). Inhibitory autophosphorylation of CaMKII controls PSD association, plasticity, and learning. Neuron *36*, 493–505.

English, J.D., and Sweatt, J.D. (1996). Activation of p42 mitogen-activated protein kinase in hippocampal long term potentiation. J. Biol. Chem. *271*, 24329–24332.

English, J.D., and Sweatt, J.D. (1997). A requirement for the mitogen-activated protein kinase cascade in hippocampal long term potentiation. J. Biol. Chem. *272*, 19103–19106.

Fanselow, M.S. (1986). Associative vs topographical accounts of the immediate shock-freezing deficit in rats: Implication for the response selection rules governing species-specific defensive reactions. Learn. Motiv. *7*, 16–39.

Frankland, P.W., Cestari, V., Filipkowski, R.K., McDonald, R.J., and Silva, A.J. (1998). The dorsal hippocampus is essential for context discrimination but not for contextual conditioning. Behav. Neurosci. *112*, 863–874.

Gerdjikov, T.V., Ross, G.M., and Beninger, R.J. (2004). Place preference induced by nucleus accumbens amphetamine is impaired by antagonists of ERK or p38 MAP kinases in rats. Behav. Neurosci. *118*, 740–750.

Guilding, C., McNair, K., Stone, T.W., and Morris, B.J. (2007). Restored plasticity in a mouse model of neurofibromatosis type 1 via inhibition of hyperactive ERK and CREB. Eur. J. Neurosci. *25*, 99–105.

Hajos, N., Nusser, Z., Rancz, E.A., Freund, T.F., and Mody, I. (2000). Cell type- and synapse-specific variability in synaptic GABAA receptor occupancy. Eur. J. Neurosci. *12*, 810–818.

Hegedus, B., Dasgupta, B., Shin, J.E., Emnett, R.J., Hart-Mahon, E.K., Elghazi, L., Bernal-Mizrachi, E., and Gutmann, D.H. (2007). Neurofibromatosis-1 regulates neuronal and glial cell differentiation from neuroglial progenitors in vivo by both cAMP- and Ras-dependent mechanisms. Cell Stem Cell *1*, 443–457.

Introini-Collison, I.B., Castellano, C., and McGaugh, J.L. (1994). Interaction of GABAergic and [beta]-noradrenergic drugs in the regulation of memory storage. Behav. Neural Biol. *61*, 150–155.

Kelleher, R.J., 3rd, Govindarajan, A., Jung, H.Y., Kang, H., and Tonegawa, S. (2004). Translational control by MAPK signaling in long-term synaptic plasticity and memory. Cell *116*, 467–479.

Kim, J.J., and Fanselow, M.S. (1992). Modality-specific retrograde amnesia of fear. Science *256*, 675–677.

Kleschevnikov, A.M., Belichenko, P.V., Villar, A.J., Epstein, C.J., Malenka, R.C., and Mobley, W.C. (2004). Hippocampal long-term potentiation suppressed by increased inhibition in the Ts65Dn mouse, a genetic model of Down syndrome. J. Neurosci. *24*, 8153–8160.

Kushner, S.A., Elgersma, Y., Murphy, G.G., Jaarsma, D., van Woerden, G.M., Hojjati, M.R., Cui, Y., LeBoutillier, J.C., Marrone, D.F., Choi, E.S., et al. (2005). Modulation of presynaptic plasticity and learning by the H-ras/extracellular signal-regulated kinase/synapsin I signaling pathway. J. Neurosci. *25*, 9721–9734.

Li, W., Cui, Y., Kushner, S.A., Brown, R.A.M., Jentsch, J.D., Frankland, P.W., Cannon, T.D., and Silva, A.J. (2005). The HMG-CoA reductase inhibitor lovastatin reverses the learning and attention deficits in a mouse model of neurofibromatosis type 1. Curr. Biol. *15*, 1961–1967.

Lindner, M.D. (1997). Reliability, distribution, and validity of age-related cognitive deficits in the Morris water maze. Neurobiol. Learn. Mem. *68*, 203–220.

Lynch, T.M., and Gutmann, D.H. (2002). Neurofibromatosis 1. Neurol. Clin. *20*, 841–865.

Martin, G.A., Viskoohil, D., Bollag, G., McCabe, P.C., Crosier, W.J., Haubruck, H., Conroy, L., Clark, R., O'Connell, P., and Cawthon, R.M. (1990). The GAP-related domain of the neurofibromatosis type 1 gene product interacts with ras p21. Cell *63*, 843–849.

McElroy, M.W., and Korol, D.L. (2005). Intrahippocampal muscimol shifts learning strategy in gonadally intact young adult female rats. Learn. Mem. *12*, 150–158.

Morris, R.G.M., Garrud, P., Rawlins, J.N.P., and O'Keefe, J. (1982). Place navigation impaired in rats with hippocampal lesions. Nature *297*, 681–683.

Nitz, D., and McNaughton, B. (2004). Differential modulation of CA1 and dentate gyrus interneurons during exploration of novel environments. J. Neurophysiol. *91*, 863–872.

North, K. (2000). Neurofibromatosis type 1. Am. J. Med. Genet. *97*, 119–127.

Rueda, N., Florez, J., and Martinez-Cue, C. (2008). Chronic pentylenetetrazole but not donepezil treatment rescues spatial cognition in Ts65Dn mice, a model for Down syndrome. Neurosci. Lett. *433*, 22–27.

Selcher, J.C., Atkins, C.M., Trzaskos, J.M., Paylor, R., and Sweatt, J.D. (1999). A necessity for MAP kinase activation in mammalian spatial learning. Learn. Mem. *6*, 478–490.

Silva, A.J., Frankland, P.W., Marowitz, Z., Friedman, E., Lazlo, G., Cioffi, D., Jacks, T., and Bourtchuladze, R. (1997). A mouse model for the learning and memory deficits associated with neurofibromatosis type I. Nat. Genet. *15*, 281–284.

Stenman, J., Toresson, H., and Campbell, K. (2003). Identification of two distinct progenitor populations in the lateral ganglionic eminence: Implications for striatal and olfactory bulb neurogenesis. J. Neurosci. *23*, 167–174.

Sweatt, J.D. (2004). Mitogen-activated protein kinases in synaptic plasticity and memory. Curr. Opin. Neurobiol. *14*, 311–317.

Wiltgen, B.J., Sanders, M.J., Ferguson, C., Homanics, G.E., and Fanselow, M.S. (2005). Trace fear conditioning is enhanced in mice lacking the {delta} subunit of the GABAA receptor. Learn. Mem. *12*, 327–333.

Xu, G.F., O'Connell, P., Viskochil, D., Cawthon, R., Robertson, M., Culver, M., Dunn, D., Stevens, J., Gesteland, R., White, R., et al. (1990). The neurofibromatosis type 1 gene encodes a protein related to GAP. Cell *62*, 599–608.

Zhu, Y., Romero, M.I., Ghosh, P., Ye, Z., Charnay, P., Rushing, E.J., Marth, J.D., and Parada, L.F. (2001). Ablation of NF1 function in neurons induces abnormal development of cerebral cortex and reactive gliosis in the brain. Genes Dev. *15*, 859–876.

Zhuo, L., Theis, M., Alvarez-Maya, I., Brenner, M., Willecke, K., and Messing, A. (2001). hGFAP-cre transgenic mice for manipulation of glial and neuronal function in vivo. Genesis *31*, 85–94.